Genetic ablation of the t-SNARE SNAP-25 distinguishes mechanisms of neuroexocytosis

Philip Washbourne[1,4], Peter M. Thompson[1,5], Mario Carta[1], Edmar T. Costa[1,6], James R. Mathews[1], Guillermina Lopez-Benditó[3], Zoltán Molnár[3], Mark W. Becher[2], C. Fernando Valenzuela[1], L. Donald Partridge[1] and Michael C. Wilson[1]

[1] *Department of Neurosciences, University of New Mexico Health Science Center, Albuquerque, New Mexico 87131, USA*

[2] *Department of Pathology, University of New Mexico Health Science Center, Albuquerque, New Mexico 87131, USA*

[3] *Department of Human Anatomy and Genetics, University of Oxford, South Parks Road OX1 3QX, UK*

[4] *Present address: Center for Neuroscience, University of California, Davis, California 95616, USA*

[5] *Present address: Department of Psychiatry, University of Texas Health Sciences Center, San Antonio, Texas 78284, USA*

[6] *Present address: Department of Physiology, Federal University of Pará, 66075-900 Belém, Pará, Brazil*

The first two authors contributed equally to this work

Correspondence should be addressed to M.C.W. (mwilson@salud.unm.edu)

Published online: 19 December 2001, DOI: 10.1038/nn783

Axon outgrowth during development and neurotransmitter release depends on exocytotic mechanisms, although what protein machinery is common to or differentiates these processes remains unclear. Here we show that the neural t-SNARE (target-membrane-associated–soluble N-ethylmaleimide fusion protein attachment protein (SNAP) receptor) SNAP-25 is not required for nerve growth or stimulus-independent neurotransmitter release, but is essential for evoked synaptic transmission at neuromuscular junctions and central synapses. These results demonstrate that the development of neurotransmission requires the recruitment of a specialized SNARE core complex to meet the demands of regulated exocytosis.

In neurons, vesicular transport and fusion are not only required for the concerted release of neurotransmitter at the active zones, but also for the delivery and insertion of material for building neuronal processes essential for establishing the multitude of connections within neural circuits. Whereas synaptic transmission is accomplished through action potential (AP)-driven neuroexocytosis, neurotransmitter is also released spontaneously, independent of action potentials both by mature neurons[1], at growth cones[2] and throughout axons[3] of developing neurons. Studies of vesicle trafficking have led to the identification of proteins required for the fusion of synaptic vesicles with the plasma membrane. In particular, a well-characterized core complex is comprised of SNAP-25, syntaxin and VAMP/synaptobrevin, termed t- and v-SNAREs to signify their location on target plasma membrane and vesicle membranes[4]. While this core complex is likely to provide a framework for a variety of protein interactions involved in assembly, fusion and recycling of synaptic vesicles (for review, see ref. 5), *in vitro* evidence indicates that the complex can promote fusion between lipid vesicles[6]. Evidence that clostridium neurotoxins abolish synaptic transmission by selectively cleaving these proteins has clearly established the critical importance of these neural SNARE proteins in stimulus-driven neurotransmitter release[7].

It remains unclear whether the same core protein machinery is used for different neuron-specific vesicular fusion events, or if their distinct functions rely on the recruitment of selective accessory proteins. The large number of SNARE family members[8] suggests that related but distinct SNAREs could contribute to the specificity of distinct membrane fusion events that occur in developing and mature synapses. However, support for such diversified roles for SNARE proteins in neuroexocytosis has been controversial. In invertebrates, mutations or neurotoxins that ablate neural SNARE expression and evoked synaptic responses do not affect synapse formation, but can lead to impairment of spontaneous synaptic activity[9–12]. In contrast, clostridium neurotoxins, which target these SNAREs, have been reported to effectively abolish both evoked and AP-independent synaptic transmission in vertebrate neurons[13]. Furthermore, constitutive exocytosis in developing axons is insensitive to tetanus toxin (TeNT), which cleaves VAMP-2, but is inhibited by botulinum neurotoxins (BoNT) A and E that target SNAP-25 (ref. 14). Other studies have reported that antisense and BoNT blockade of SNAP-25 expression inhibit neurite outgrowth[15–17]. These findings advocate the involvement of an alternative v-SNARE, such as Ti-VAMP[18], in membrane fusion for axon elongation, but raise the possibility that SNAP-25 could have a common role in all forms of neuroexocytosis.

Here we examined the involvement of SNAP-25 in neuronal exocytosis by generating *Snap25* null mutant mice. Our results show that this mutant's nervous system develops normally

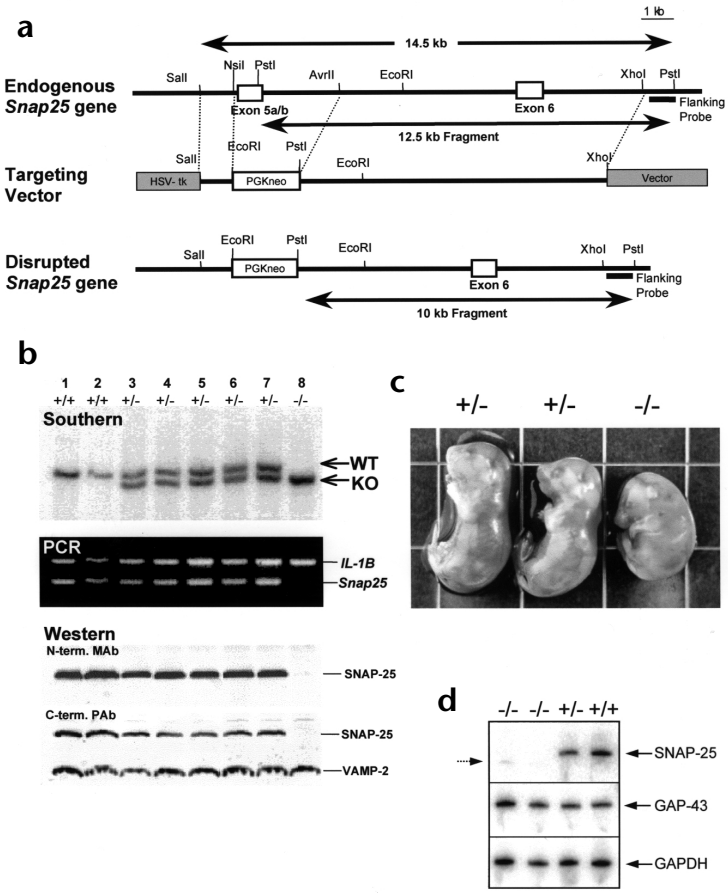

Fig. 1. The *Snap25*$^{-}$ mutation abolishes expression of SNAP-25 protein. (**a**) Targeting construct was generated from a genomic clone containing exons 5 and 6 in which the region containing both exon 5a and 5b defined by *Nsi*I and *Avr*II sites was replaced by PGKneo. The 3′ flanking *Xho*I/*Pst*I fragment was used in Southern blots to distinguish the 10-kb *Pst*I fragment of the disrupted *Snap25* gene, compared to the endogenous 12.5-kb fragment. (**b**) Southern blot analysis and genomic PCR distinguish the phenotypes of fetuses within a representative litter by restriction fragment length and SNAP-25 PCR product comparison to IL-β1, another chromosome 2 gene (top). Western blot analysis demonstrates the lack of SNAP-25 protein using N-terminal and C-terminal antibodies to SNAP-25 (bottom). (**c**) The characteristic gross morphology *Snap25*$^{-/-}$ fetuses at E17.5–18.5 distinguishes the mutants from normal littermates. In addition to their immobile stature, the mutant fetuses are smaller than normal littermates (*Snap25*$^{+/+}$, 1.270 g; *Snap25*$^{+/-}$, 1.264 g; *Snap25*$^{-/-}$, 1.151 g; n = 3, 3, 2, respectively, from one E18.5 litter). (**d**) RNA analysis by RT-PCR demonstrates a lack of SNAP-25 expression, confirming that the exon 5a/5b deletion results in a null mutation. The low level (1–2% wild type) of truncated transcript (broken arrow) corresponds to an exon 5-less transcript.

in utero, despite the lack of this component of the neuronal SNARE complex. Moreover, we find that axonal outgrowth, targeting of synaptic contacts, and AP-independent, spontaneous transmitter release can occur, although AP-dependent release is completely abolished. Our results suggest that the vesicular fusions necessary for membrane addition, neurite outgrowth and for stimulus-independent synaptic activity proceed by mechanisms distinct from those used in Ca^{2+}-triggered synaptic transmission.

Results

Fetal development of SNAP-25-deficient mice

SNAP-25-deficient mice were generated by gene targeting using a vector that replaced the alternatively spliced exons 5a and 5b (ref. 19), and the 5′ portion of the downstream intron with a PGK-neo^{r} gene cassette (**Fig. 1a**, and Supplementary methods, available on the *Nature Neuroscience* web site). Exons 5a/5b encode residues Glu_{56}–Arg_{94} that are required for direct interaction with syntaxin 1 (ref. 20) and contribute to the four barrel helix formed in the ternary SNARE core complex[21]. These exons also encode alternative motifs of four conserved cysteine residues that are sites of palmitoylation[22] that can provide an intrinsic membrane anchor[23,24] and have a direct role in recycling the core complex components after membrane fusion and neurotransmitter secretion[25].

Mice heterozygous for the *Snap25* mutation were robust, fertile and phenotypically indistinguishable from wild-type littermates. In contrast, no homozygous mutants were obtained from heterozygote crosses, consistent with an embryonic lethal phenotype. At early stages of fetal development (embryonic day (E) 10.5 and 13.5), the homozygous mutants were indistinguishable at a gross morphological level, and at E17.5–18.5 the mutants were recovered at the expected Mendelian ratio (0.248, 0.502, 0.248 homozygote mutant, heterozygote and wild-type, respectively; n = 205). At this stage, homozygous mutant fetuses were readily distinguished by their characteristic tucked position, smaller size (**Fig. 1c**), and failed to exhibit either spontaneous movement or sensorimotor reflexes in response to mechanical stimuli. Despite the clear loss of neuromuscular function, E18.5 mutants had a beating heart and all internal organs appeared intact and appropriately located. However, the mutants often had an external blotchy appearance, suggesting an underlying vascular abnormality of the skin. These hyperemic blotches likely correlate with numerous dilated vascular channels found in the subcutaneous soft tissue of the *Snap25*$^{-/-}$ fetuses (**Fig. 3d**, arrowhead). Examination of mutant diaphragms (see below) showed that while muscle fibers are innervated by the respiratory phrenic nerve, they failed to exhibit stimulus-evoked contraction, suggesting that the lethality at birth is a consequence of respiratory failure.

Western blot analysis of brain proteins showed a dose-dependent loss of SNAP-25 protein in heterozygote and homozygote mutants (**Figs. 1b** and **2b**). Comparable results were obtained both with a polyclonal antibody to the C-terminal peptide sequence and a monoclonal antibody SMI-81 that detects an epitope within the N-terminal 31 residues (P.W., data not shown). Based on the genomic sequence, abnormal splicing of exon 4 to 6 in the absence of exon 5 should lead to a shift in open reading frame with termination after one codon into exon 6, and translation of a 55 residue, 6.326-kD polypeptide. SNAP-25 mRNA, however, was not detectable by northern blots of mutant total brain RNA (data not shown) and reverse transcriptase-polymerase chain reaction (RT–PCR) analysis, within the linear range of amplification, revealed only low amounts of slightly shorter SNAP-25 transcripts corresponding to 1–2% of that found in wild type (**Fig. 1d**). After excessive amplification (35 cycles), these transcripts were mapped with restriction enzymes and found to be consistent with an exon 4/6 spliced RNA (data not shown). Western blot analysis of low molecular weight proteins using the N-terminal MAb, however, failed to detect a SNAP-25 polypep-

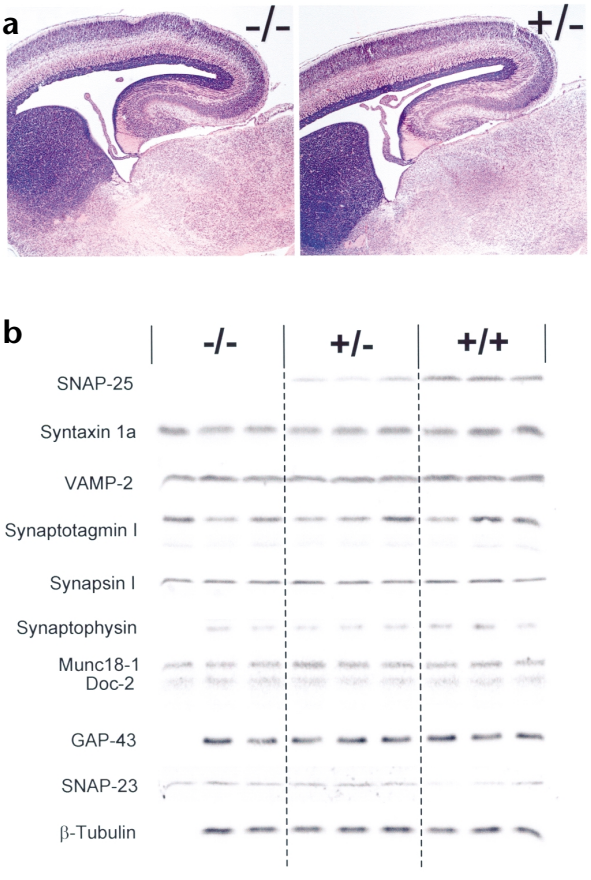

Fig. 2. Brain structure and synaptic protein levels appear normal in *Snap25*$^{-/-}$ mice. (**a**) Parasagittal sections of cortex and hippocampus stained with hematoxylin and eosin shows normal morphology of *Snap25*$^{-/-}$ mutant brain. (**b**) Western blot analysis of E17.5 forebrain shows no dramatic differences in levels of expression of synaptic proteins. Only 2 samples of *Snap25*$^{-/-}$ proteins were probed with antibodies to synaptophysin, GAP-43 and β-tubulin. Importantly, SNAP-23, the non-neuronal homolog of SNAP-25, is not significantly induced in the *Snap25* null mutant brain.

tide of ~6 kD, confirming that neither the abnormally spliced mRNA nor the truncated polypeptide accumulate to a significant level in mutant fetal brain. Based on these observations, we conclude that the *Snap25* exon5a/5b deletion results in a null mutation, which we designate *Snap25*$^{-}$.

Brain development proceeds normally

Major brain structures including the hippocampus and neocortex were morphologically normal in *Snap25*$^{-/-}$ embryos compared with wild-type and *Snap25*$^{+/-}$ embryos (**Fig. 2a**). A survey of presynaptic proteins revealed no detectable difference in the expression among wild-type, heterozygote and homozygous mutants (**Fig. 2b**). There was also no apparent change in the level of SNAP-23, the non-neuronal homolog of SNAP-25 (ref. 26). Because SNAP-23 is expressed at much lower levels than SNAP-25 in neurons[27], we cannot entirely exclude the possibility of a small increase of SNAP-23 among neuronal cell populations that could be obscured by the contribution of non-neuronal cells of the developing brain. These data indicate that the *Snap25* loss-of-function mutation does not result in major compensatory changes in expression of other proteins that are prominent mediators of presynaptic function.

Histological examination of hematoxylin- and eosin- or cresyl-violet-stained paraffin sections taken from E17.5 and E18.5 *Snap25*$^{-/-}$ brains showed no evidence for appreciable cellular deficits. Comparable cell densities were observed in neocortex of mutant and wild-type fetuses (**Fig. 3a** and **b**) and the diencephalon and brainstem of the mutants (**Fig. 3c**) showed no apparent cellular or architectural defects. Moreover, tyrosine hydroxylase immunocytochemistry (**Fig. 3c**, inset), a marker for mature catecholaminergic neurons, demonstrated a normal pattern of immunoreactivity in the *Snap25*$^{-/-}$ brainstem. This differs from the marked cell loss reported for *munc18-1/nsec-1* mutants[28] and suggests that the lack of SNAP-25 results in a more subtle phenotype, possibly acting downstream of *munc18-1* mediated function(s) in neurotransmitter release. This is likely due to the persistence of spontaneous release of neurotransmitter in SNAP-25 deficient embryos (see below) that is entirely abolished in the *munc18-1* mutant.

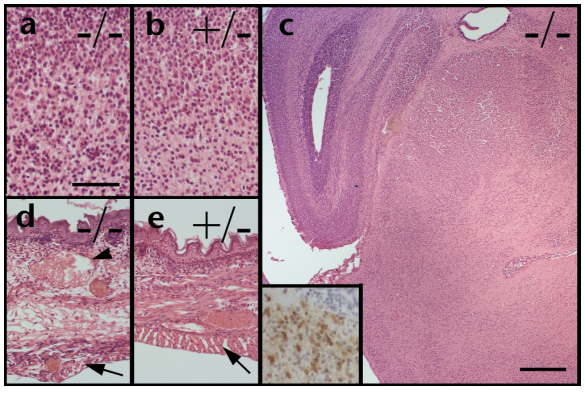

Spontaneous but not stimulus-driven release at NMJs

The normal appearance of fetal brain development in SNAP-25 mutants suggested that processes that accompany neuronal differentiation, especially initial neurite formation and outgrowth, and possibly initial synapse formation, may occur without SNAP-25-mediated neuroexocytosis. To examine this question, we first evaluated the neuromuscular junction synapse *in situ* in the fetal diaphragm. Fluorescent immunohistochemistry of whole-mount preparations stained with syntaxin 1a antibodies (**Fig. 4a**) demonstrated phrenic nerve innervation of the diaphragm in *Snap25*$^{-/-}$ late-stage (E17.5–18.5) fetuses. Fluorescently labeled α-bungarotoxin (α-Bgt) also readily distinguished acetylcholine receptor (AChR) clusters in the muscle that closely matched the pattern of syntaxin-positive fibers and colocalized with axon terminals (**Fig. 4a**, inset). However, the overall pattern of synaptic sites seen with

Fig. 3. Histopathological examination of SNAP-25-deficient fetuses. The neocortex (**a**, **b**), hippocampus, thalamus, and midbrain (**c**) are normally developed in E19 null mutant mice as compared to *Snap25*$^{+/-}$ littermate controls. The midbrain of the *Snap25*$^{-/-}$ mutant fetus is well populated by tyrosine hydroxylase immunoreactive neurons (**c**, inset). (**d**, **e**) The dermis of knockout mice contains large ectatic vascular channels (arrowhead, anterior chest wall) not found in *Snap25*$^{+/-}$ or wild-type (data not shown) fetuses. In addition, the subcutaneous musculature (arrows) is sparse and disorganized in mutant mice. (**a–e**) Hematoxylin and eosin; (**c**, inset) anti-tyrosine hydroxylase DAB stain. Scale bars, 50 μm (**a**, **b**, **d**, **e**, inset **c**), 250 μm (**c**).

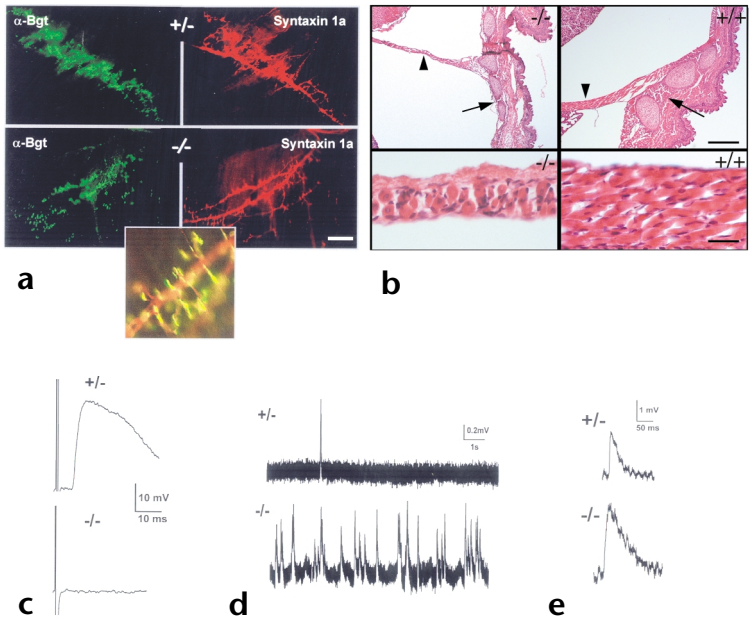

Fig. 4. The NMJ is formed in *Snap25* mutants, but does not show ACh release. (**a**) Diaphragms from E17.5–18.5 fetuses were stained with Oregon-Green-labeled α-bungarotoxin (α-Bgt) and a rabbit polyclonal to syntaxin 1a. Note the more diffuse pattern of axons (red) and stained endplates (green) in *Snap25*$^{-/-}$ compared with heterozygote (*Snap25*$^{+/-}$) controls. Scale bar, 200 μm. Inset below shows an overlay of *Snap25*$^{-/-}$ mutant neuromuscular junctions to demonstrate colocalization (yellow) of axon terminals with clustered AchRs. Scale bar, 20 μm. (**b**) Paraffin sections of E19 fetuses stained with hematoxylin and eosin demonstrate that diaphragms (arrowheads) and intercostal muscles (arrows) of *Snap25*$^{-/-}$ mice (left) are thin and contain fewer myofibers than wild-type littermates (*Snap25*$^{+/+}$, right). The anterior attachment of the diaphragm to the thoracic wall (top) is markedly abnormal in the mutant fetus. Higher magnification of the mid-portion of the same diaphragms (bottom) shows the decrease in the number of myofibers and thickness of the structure. Scale bars, 100 μm (top), 250 μm (bottom). (**c**) Intracellular recordings of responses from diaphragm muscle following a 0.2-ms suprathreshold stimulus to the phrenic nerve illustrate the complete lack of evoked response at mutant NMJs. (**d**) Recordings of spontaneous events in the presence of 600 nM TTX demonstrate increased frequency of mEPPs in *Snap25*$^{-/-}$ NMJs. (**e**) Traces of representative mEPPs show increased amplitude of these spontaneous synaptic events in *Snap25* mutants.

both syntaxin and α-Bgt staining of AChR clusters appeared more dispersed in *Snap25*$^{-/-}$ mutants compared to the dense midline localization in heterozygote or wild-type littermates. Histological examination of diaphragm cross-sections showed that in contrast to the multilayered, highly packed muscle of normal diaphragms (**Fig. 4b**), the muscle fibers of the *Snap25*$^{-/-}$ diaphragms were less numerous comprising approximately one-half the thickness of normal diaphragms. This suggests that the decreased number of muscle fibers may correlate with the more disarrayed appearance of innervation and localization of synaptic sites. In addition, the intercostal muscles (**Fig. 4b**, arrows) and anterior chestwall musculature (**Fig. 3d**, arrow) of *Snap25*$^{-/-}$ embryos were also thin and disorganized.

To compare synaptic transmission in SNAP-25-deficient and normal NMJs, evoked and spontaneous AP-independent postsynaptic responses were recorded. Phrenic nerve stimulation of *Snap25*$^{+/+}$ and *Snap25*$^{+/-}$ diaphragms invariably produced evoked endplate potentials (EPPs; **Fig. 4c**) and muscle contraction (3/3 and 13/13 diaphragms, respectively). In contrast, diaphragms from SNAP-25-deficient mice showed neither EPPs nor evoked contraction (0/16 diaphragms). Mutant diaphragms, however, contracted vigorously after application of 1 mM carbachol, indicating that nicotinic receptors detected by α-Bgt are functional (*Snap25*$^{-/-}$, 6/6 ; *Snap25*$^{+/-}$, 6/6).

Unexpectedly, spontaneous miniature endplate potential (mEPP) activity was consistently recorded in *Snap25*$^{-/-}$ mutant diaphragms (**Fig. 4d** and **e**). While the mean frequencies were comparable, the frequency distributions of mEPPs obtained from individual fetuses showed considerably greater variability in *Snap25*$^{-/-}$ diaphragms than those from normal littermates ($p < 0.05$, Levene's *F*-test; **Table 1**). The mean amplitude of mEPPs was more than twofold greater in *Snap25*$^{-/-}$ diaphragms, whereas the decay of the mEPPS was not significantly different ($p < 0.005$ and $p > 0.05$, Mann–Whitney test, respectively). Consistent with acetylcholine release drawn from an accessible pool of vesicles[29], the frequency of mEPPs in mutant diaphragms could be increased further by application of α-latrotoxin, although the response to the toxin was variable among preparations (data not shown).

These data established that for the NMJ, axons were able to establish synapses *in vivo* that exhibit spontaneous AP-independent neurotransmitter release through a SNAP-25 independent secretory event, but that this mechanism was incapable of supporting evoked responses. The difference observed in the amplitude of TTX-resistant mEPPs is not likely dictated by a structural property of the muscle, as individual mutant and control myotubes had comparable diameters (**Fig. 4b**). An initial characterization of mutant NMJs has revealed larger endplate diameters and markedly lower levels of acetylcholinesterase (R. Silva, L.D.P., M.C.W., unpublished observations), which could contribute to the greater mEPP amplitude. In contrast, the increased frequency of mEPPs seen at mutant NMJs strongly suggests a presynaptic site of action that may reflect stockpiling of vesicles in terminals that lack a mechanism for evoked synaptic transmission.

Table 1. Action potential-independent, spontaneous responses in diaphragm of normal and mutant mice.

	Amplitude (mV)		Decay τ (ms)		Frequency (s^{-1})	
	normal	mutant	normal	mutant	normal	mutant
mean ± s.e.m.	1.87 ± 0.33	4.66 ± 1.07	24.60 ± 3.68	35.12 ± 4.30	0.016 ± 0.0041	0.094 ± 0.047
Mann–Whitney	$p = 0.0047$		$p = 0.053$		$p = 0.377$	
Levene	$p = 0.178$		$p = 0.372$		$p = 0.008$	

mEPPs were recorded in diaphragms of normal (n = 3 +/+; 7 +/–) and homozygote *Snap25*$^{-/-}$ mutants (n = 11) E17.5–18.5 fetuses. Data are given as means ± s.e.m. A Kolmogorov–Smirnov test indicated that amplitude and frequencies were not consistent with a normal distribution. The Mann–Whitney test was used to compare medians and the Levene test, to compare variances of data from normal and mutant diaphragms.

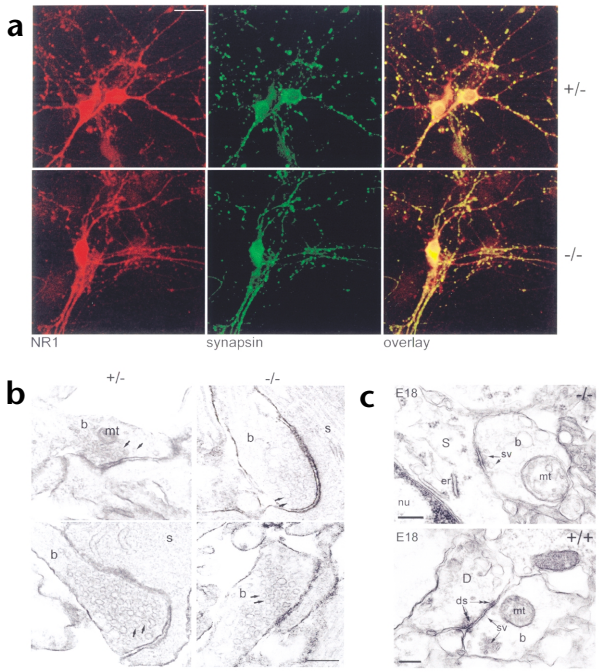

Fig. 5. *Snap25*$^{-/-}$ central neurons exhibit normal synaptic morphology both in culture and *in vivo*. (**a**) Hippocampal cells were stained for NMDA receptor subunit (NR1, red) and synapsin (green) at 7 d.i.v. The merged confocal images (overlay) demonstrate colocalization of the postsynaptic NR1 with presynaptic synapsin as yellow punctate staining corresponding to putative synapses. Electron micrographs of hippocampal neurons obtained from E18.5 brain cultured for 7 d.i.v. (**b**) and from E18.5 cortex (**c**) demonstrate immature synapses in both normal (+/– or +/+) and homozygous null mutants (–/–) with accumulations of synaptic vesicles (arrows) and parallel opposed synaptic membranes. S, soma; D, Dendrite; b, bouton; ds, desmosome; mt, mitochondria; nu, nucleus; er, rough endoplasmic reticulum. Scale bars, 20 μm (**a**); 200 nm (**b**, **c**).

Neurite outgrowth and synaptic function in CNS

To investigate neurotransmission in central nervous system neurons, hippocampal and cortical cultures were prepared from E17.5–18.5 fetuses. Immunofluorescent staining for NMDA receptor subunit NR1 and synapsin showed that mutant neurons exhibited considerable neurite outgrowth after seven days in culture (7 days *in vitro*; d.i.v.), comparable to cultures derived from normal littermates (**Fig. 5a**, and data not shown). Merged images demonstrate colocalized punctate staining consistent with synaptic contacts formed between pre- and postsynaptic terminals. Electron microscopy also revealed abundant but immature synapses on processes of both *Snap25*$^{-/-}$ and normal cultured neurons (**Fig. 5b**). Mutant neurons at DIV 8-10, however, showed a loss of VAMP-2 positive processes seen at d.i.v. 5–7 that was followed by further apparent degeneration (data not shown), and prohibited analysis of more mature synaptic contacts. This was not prevented by addition of either 25 μM glutamate or 0.25 μM AMPA to promote synaptic activity or 25 mM KCl to maintain the cells in a depolarized state, suggesting that SNAP-25-deficient neurons may be unable to provide sufficient secretion of neurotrophic or other factors. Electron micrographs showed the presence of immature synapses in E18.5 *Snap25*$^{-/-}$ fetal cortex (**Fig. 5c**), demonstrating that synapse formation also occurs without SNAP-25 *in vivo*.

Whole-cell patch clamping of SNAP-25-deficient hippocampal neurons revealed spontaneous miniature excitatory postsynaptic currents (mEPSCs) in the presence of TTX (**Fig. 6a**). Whereas the amplitude of mEPSCs in *Snap25*$^{-/-}$ neurons did not differ from *Snap25*$^{+/-}$ cultures (*Snap25*$^{-/-}$, 6.5 ± 1.4 pA, $n = 12$; *Snap25*$^{+/-}$, 9.0 ± 3.0 pA, $n = 7$; $p > 0.35$, Student's *t*-test), the frequency of these events was on average lower in mutant neurons, although there was some variability between individual neurons (*Snap25*$^{+/-}$, 2.2 ± 1.2 Hz, $n = 7$; *Snap25*$^{-/-}$, 0.22 ± 0.04 Hz, $n = 13$; $p = 0.04$; Student's *t*-test), consistent with a decreased number of functional synaptic contacts between mutant neurons. The frequency of mEPSCs from *Snap25*$^{-/-}$ neurons was stimulated dramatically by α-latrotoxin that accelerates the rate of spontaneous synaptic vesicle fusion events[30]. Moreover, application of glutamate agonists showed that postsynaptic responses were unaffected in SNAP-25-

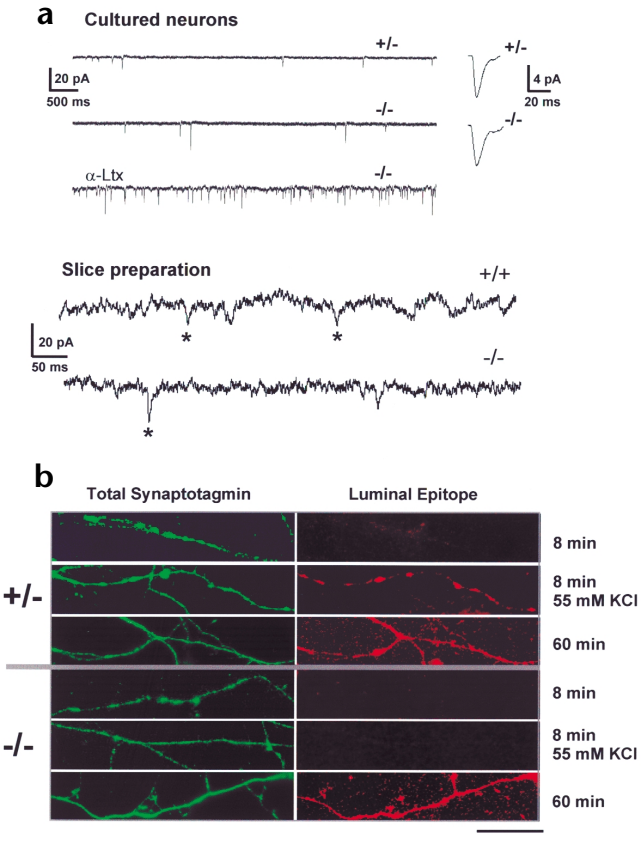

Fig. 6. Spontaneous, AP-independent neurotransmission, constitutive exo-/endocytosis, but not evoked neuroexocytosis in *Snap25*$^{-/-}$ neurons. (**a**) Cultured hippocampal neurons at 7 d.i.v. and cortical neurons in E18.5 brain slices from homozygote mutants display mEPSCs. Top two traces show voltage-clamped, whole-cell patch recordings of mEPSCs from heterozygote and homozygous mutant neurons; average mEPSCs (*Snap25*$^{+/-}$, $n = 86$ events; *Snap25*$^{-/-}$, $n = 61$ events) are depicted to the left. Third trace (α-Ltx) demonstrates the stimulation of mEPSCs from *Snap25*$^{-/-}$ neurons by 3 nM α-latrotoxin. Bottom set of traces shows recordings of mEPSCs (asterisks) from E18.5 cortical slices of *Snap25*$^{+/+}$ ($n = 23$ events, 92 s, 9.1 ± 0.58 pA) and *Snap25*$^{-/-}$ neurons ($n = 14$ events, 52 s, 9.2 ± 1.06 pA). (**b**) Hippocampal cultures were assayed at 7 d.i.v. by incubating with a synaptotagmin lumenal PAb (red) and subsequent fixation and staining for total synaptotagmin I (green). SNAP-25 null mutant neurons retain constitutive exocytosis seen after 60 min, but do not exhibit depolarization-driven exocytosis (8 min, 55 mM KCl). Scale bar, 10 μm.

deficient neurons (100 μm kainate, *Snap25*$^{-/-}$, 13 ± 3 pA/pF; *Snap25*$^{+/-}$, *Snap25*$^{+/+}$, 21 ± 4 pA/pF, $n = 8$; 100 μM NMDA/10 μM glycine, *Snap25*$^{-/-}$, 16 ± 5 pA/pF; *Snap25*$^{+/-}$, *Snap25*$^{+/+}$, 16 ± 3 pA/pF, $n = 9$). mEPSCs were also recorded from cortical slices of *Snap25*$^{-/-}$ E18.5 embryos (**Fig. 6a**, bottom traces) indicating that, as mutant NMJs, immature CNS synapses formed *in vivo* and seen *in situ* at the ultrastructural level are functional.

To determine whether *Snap25*$^{-/-}$ central synapses were able to exhibit stimulus-evoked neuroexocytosis, we assessed coupled exocytosis/endocytosis using antibodies to the luminal domain of synaptotagmin I (syt-ecto Abs) to label synaptic vesicle membrane fusion[31]. Endocytosis was clearly detectable in *Snap25*$^{+/-}$ neurons after KCl depolarization-evoked exocytosis (8 min, 55 mM KCl; **Fig. 6b**, upper panels), as well as after prolonged exposure to the antibody to measure membrane recycling in the absence of depolarization (60 min). Labeling *Snap25*$^{-/-}$ neurons for 60 minutes in the absence of depolarization revealed constitutive vesicle cycling (**Fig. 6b**, lower panels), comparable to heterozygote (**Fig. 6b**, upper panels), and wild-type neurons (data not shown). In contrast, *Snap25*$^{-/-}$ neurons failed to exhibit KCl depolarization-dependent uptake of syt-ecto Abs, suggesting that there was a block in regulated exocytosis required for stimulus-dependent neurotransmission.

Discussion

Our findings for a selective role for SNAP-25 in evoked, Ca^{2+}-triggered neurotransmission raises several questions about the mechanisms, molecular components and composition of SNARE core complexes that orchestrate vesicular transport and fusion at different stages of neuronal development. In their classic study of synaptic transmission at the neuromuscular junction, del Castillo and Katz[32] used a statistical argument to demonstrate that the unit that underlies evoked release is identical to the unit of spontaneous release. They used the term all-or-none quantal unit to describe this basic element of synaptic transmission. At least in the case of the NMJ, there is considerable evidence to associate the structure of the quantal unit with the synaptic vesicle (for example, see ref. 33). There is, however, less evidence to inexorably associate the mechanism of evoked quantal release with the mechanism of spontaneous quantal release. Here we have described a mutation of the presynaptic machinery in which the probability of evoked release is essentially zero and yet spontaneous quantal release occurs. This provides strong evidence that evoked release and spontaneous quantal release do not necessarily proceed by a similar mechanism. Such a mechanistic change may reflect the need for different SNARE complexes to recruit a collection of accessory proteins to provide the necessary trigger and barriers to promote membrane fusion in response to stimulus-driven localized high $[Ca^{2+}]_i$ that underlies synaptic transmission for mature nervous system function.

Previous studies using botulinum neurotoxins and antisense oligonucleotide inhibition implicated the involvement of SNAP-25 in the exocytotic machinery mediating constitutive vesicular fusion for neurite extension[15–17], as well as for AP-independent exocytosis[14] and neurotransmitter release[13]. Our results clearly show, however, that SNAP-25 null mutant neurons are able to develop neurite processes in culture and to effectively extend axons to their targets *in vivo*, both at the periphery to form NMJs (**Fig. 4**), and centrally within the brain (**Figs. 2** and **3**, Z.M., J. Small, J.M., C. Blakemore and M.C.W., unpublished data). One explanation for the apparent discrepancy between the neurotoxin and genetic experiments is that fragments produced by BoNT/A or E may exert a dominant negative effect on constitutive exocytosis by blocking vesicular fusion directly[34] or by sequestering components of the fusion machinery into non-functional complexes. For example, C-terminal truncated forms of SNAP-25 generated by neurotoxin cleavage are able to form a ternary complex with syntaxin and VAMP but are unable to promote fusion[35,36] which could interfere with assembly and recycling of components needed for constitutive exocytosis and neurite outgrowth.

Another possibility is that compensation by either SNAP-23, or perhaps another mechanistically related protein, could occur in response to the null mutation but not by acute blocks imposed by BoNT or antisense oligonucleotides. The lack of a substantial increase in SNAP-23 expression argues against an upregulatory response at least for this SNAP-25 homolog. In addition, it is unlikely that compensation could support only axonal outgrowth, initial targeting and synapse formation, and AP-independent release, but not be applied to stimulus-driven synaptic transmission. Taken together, these observations suggest that a more generalized exocytotic core complex mediates vesicle fusion before the commitment of fusion machinery to confer AP-dependent release of neurotransmitter. Although both innervation and AChR clusters are more widely distributed in the diaphragms of the mutants, they form functional synapses, indicating that AP-independent release mechanisms may be sufficient to provide neural-derived signal(s) for the initial refinement and patterning of neuromuscular synapses[37,38].

The deficits produced by the SNAP-25 null mutation can be considered in view of mutations of other known presynaptic proteins, for example the phenotypes produced by targeted mutation of nsec1/munc18 (ref. 28) and synaptotagmin[39]. Munc18-1 interacts with syntaxin 1a in its 'closed' conformation[40], which is thought to stabilize the structure of syntaxin and promote an initial stage in assembly of exocytotic machinery before formation of the ternary complex with SNAP-25 and VAMP[5]. Munc18-1-deficient mutants, which, like *Snap25* mutants, are immobile and die at birth, lack both AP-independent and evoked release mechanisms, and despite apparently normal initial morphological development and formation of axonal pathways exhibit profound neuronal loss in several brain regions[28]. This suggests that, in the absence of munc18-1, syntaxin 1a (or the closely related syntaxin 2 or 3) may be unable to be recruited into an initial and perhaps general step in assembly of the core complexes capable of mediating either AP-dependent or AP-independent neurotransmitter release. SNAP-25-deficient neurons, on the other hand, can assemble synaptic machinery necessary for spontaneous release, but fail to develop stimulus-evoked release, indicating that the core complex assembled without SNAP-25 is not equipped for mature regulated exocytosis. In contrast, synaptotagmin I seems to be required late in the exocytotic process at a point immediately before membrane fusion where it likely serves as a calcium sensor[39]. Synaptotagmin I null mutants are initially viable at birth, exhibit neuromuscular responses, but ultimately fail to perform coordinated behaviors such as suckling. Synaptotagmin deficient neurons show a specific deficit in the synchronous, fast Ca^{2+}-dependent component of evoked transmission that presumably underlies such complex activities, while retaining the slow component, as well as spontaneous synaptic activity[39]. SNAP-25 has been shown to interact directly with synaptotagmin[41], and therefore, in addition to being central in forming a core SNARE complex, may serve in the recruitment of this calcium sensor to the site of membrane fusion. Thus, each of these mutations appears to dissect a different point in the developmental specialization and temporal order of molecular events required for neurotransmission.

Because axonal outgrowth proceeds in the absence of SNAP-25 or munc18-1 (ref. 28) and is resistant to TeNT[14], precluding the involvement of VAMP-2, we suggest that SNARE complexes responsible for constitutive membrane fusion required for the construction of axon processes involve non-neuronal and more generalized members of the SNAP-25, syntaxin and VAMP gene families. Similarly, the utilization of more generalized SNARE components may also underlie AP-independent spontaneous secretion in which the position of SNAP-25 may be held by a homologous SNARE, possibly SNAP-23. The diversity of the composition of the SNARE complex thus may reflect the need to distinguish ongoing vesicle fusion for axonal outgrowth and spontaneous neurotransmitter release from the fusion machinery that is equipped and likely to trigger synaptic exocytosis. For example, spontaneous neurotransmitter release could provide for specific signaling in the morphological development of postsynaptic dendrite spines and in synaptic plasticity[42].

Our results provide genetic evidence that the neuronal SNARE protein SNAP-25, a constituent of the exocytosis complex present in mature presynaptic nerve terminals, is specifically responsible for evoked synaptic transmission, but is not essential for AP-independent, spontaneous release of neurotransmitter or process outgrowth and axonal elongation during neural development. Recently, it was reported that cultured neurons from synaptobrevin/VAMP-2 null mutant mice also exhibit spontaneous synaptic transmission (although at much reduced frequency) in the absence of evoked responses[43]. It was suggested that such Ca^{2+}-independent spontaneous activity from neurons, which must establish and maintain synapses *in vivo*, could reflect exocytosis in the absence of SNARE complexes. Whereas our results indicate AP-independent activity may not be comparably reduced at synapses formed *in situ*, these studies underscore the need to define the molecular mechanism that drives membrane fusion for spontaneous neurosecretion, and to establish what role this may have in synapse formation and, ultimately, for activity-dependent neurotransmission. Together with other mutants targeting presynaptic proteins, SNAP-25-deficient mice will provide an important means to resolve the complex protein assemblies required for these different acts of neuroexocytosis in development and in mature nervous system function.

Methods

Mutant mice. The *Snap*25 null mutation was generated by targeted gene replacement in embryo stem cells using standard positive-negative selection procedures[44]. SNAP-25 coding sequence was disrupted in the gene targeting construct (p4.2) by replacing both exons 5a and 5b with PGK-neo (for details and genotyping, see **Fig. 1a** and Supplementary methods). For the studies reported, littermates at E17.5–18.5, judged by the morning of the plug, were obtained from mice backcrossed onto a C57BL/6J background for 4–5 generations. Studies were done in accordance with guidelines of the University of New Mexico HSC Laboratory Animal Care and Use Committee and the NIH.

Western blotting and RT-PCR. Fetal brain extracts were prepared by homogenization in 0.32 M sucrose, 20 mM Tris pH 7.4, 1 mM DTT, 1% Nonidet P-40 and protease inhibitors (Complete Minitablet, Boehringer-Mannheim, Indianapolis, Indiana). The detergent extracts were centrifuged, and protein concentration of the solubilized protein was determined with Micro BCA assay kit (Pierce, Rockford, Illinois). Equal amounts of protein were loaded on polyacrylamide gels, transferred to nitrocellulose and probed with the antibodies to the following proteins: SNAP-25 C-terminus and N-terminus (Sternberger Monoclonals, Lutherville, Maryland), VAMP-2 (gift from C. Montecucco, Univ. of Padova, Italy), syntaxin 1 (Sigma, St. Louis, Missouri), synaptotagmin 1 (Wako, Richmond, Virginia), synapsin 1 (Synaptic Systems, Göttingen, Germany), Munc18-1, Doc-2 (BD Transduction Laboratories, Lexington, Kentucky), synaptophysin, GAP-43 (Boehringer-Mannheim), SNAP-23 (gift from A. Klip, The Hospital for Sick Children, Toronto, Ontario) and β-tubulin (Chemicon, Temecula, California). Primary antibodies were detected with either anti-mouse ^{125}I-labeled IgG, or anti-rabbit HRP conjugated IgG followed by chemiluminescence assay (ECL-Plus, Amersham Pharmacia, Piscataway, New Jersey) and quantitated on a STORM PhosphoImager system (Molecular Dynamics, Sunnyvale, California). RT-PCR was done on RNA extracted with guanidinium thiocyanate and phenol:chloroform using the Titan RT-PCR 1 tube system (Boehringer-Mannheim) with ^{32}P-dCTP added as a tracer, and primers to the start and stop codons of SNAP-25 coding sequence. Amplification was limited to 22 cycles to be in the linear range of the reaction and the products were electrophoresed in 8% polyacrylamide gels and visualized by phosphoimaging.

Histology, immunohistochemistry and electron microscopy. Fetal brains were dissected and fixed by immersion in 4% paraformaldehyde/0.1 M phosphate buffer, pH 7.4 for 24 h. Whole embryos were fixed in 10% formalin. Brains or whole fetuses were paraffin embedded, sectioned at 8 μm and stained with hematoxylin and eosin, cresyl violet, or tyrosine hydroxylase antibodies (Boehringer-Mannheim). Diaphragms were fixed by immersing in 2% paraformaldehyde/0.1 M phosphate buffer for 1 h, and permeablized with 1% Triton X-100 (ref. 45). AChRs were visualized by staining with Oregon green labeled α-bungarotoxin (Molecular Probes, Eugene, Oregon) and axons with rabbit anti-syntaxin 1 (gift C. Montecucco, Univ. of Padova, Italy). Vesicle cycling was assayed essentially as described previously[14]. Briefly, cortical neuronal cultures were either incubated with anti-synaptotagmin antibody, syt-ecto Ab (gift from P. De Camilli, Yale University) as indicated before fixation or fixed directly with 4% paraformaldehyde and 4% sucrose for 20 min at 37°C. Cells were treated with 0.2% Triton-X-100, 4% normal donkey and goat serums, washed with PBS, and incubated with secondary antibodies conjugated to FITC or Cy3 (Jackson Immunochemicals, West Grove, Pennsylvania) for fluorescence microscopy. For dual-fluorescent confocal microscopy, neuron cultures were fixed with methanol and stained with monoclonal antibodies to NMDA receptor subunit 1 (PharMingen, San Diego, California) and polyclonal antibodies to synapsin (Chemicon), visualized with Cy3 and Cy2-labeled secondary antibodies, respectively, and viewed using an Olympus Fluroview IX70 confocal microscope. Confocal images were displayed using Adobe Photoshop.

For electron microscopy of synapses, brains obtained from E18.5 fetuses were fixed in 2% paraformaldehyde/2% glutaraldehyde, and cortical cells were fixed with 3% glutaraldehyde. Further fixation with OsO_4, and uranyl acetate staining were performed by standard techniques. (See Supplementary methods for details.)

Electrophysiology. Postsynaptic responses from dissected diaphragms were recorded at room temperature as described[46]. For evoked responses, a 0.2-ms suprathreshold stimulus was applied to the phrenic nerve using a suction electrode, while mEPPs were recorded in 600 nM TTX without phrenic nerve stimulation. mEPP amplitudes were linearly adjusted to $E_m = -75$ mV before comparing data from different cells. Decay time constants were only calculated where the mEPP decay could be clearly fit by a single exponential curve. No differences were seen between homozygous wild-type and heterozygous genotypes, and the data were pooled as normal NMJ responses.

Vibratome coronal sections from E18.5 embryos were pre-incubated for 45 min at 37°C in Krebs bicarbonate buffer containing 0.5 mM Ca^{2+} and 10 mM Mg^{2+} equilibrated with O_2/CO_2 (95:5) and then in standard Krebs bicarbonate buffer for 30–60 min as described[47]. Cortical neurons were visualized with infrared differential interference contrast using an Olympus BX50WI microscope. In all cases, neuronal currents were measured in the whole-cell patch-clamp configuration as described[48]. (See Supplementary methods for details.) The internal solution contained 4 mM NaCl, 0.4 mM $CaCl_2$, 5 mM EGTA,10 mM HEPES, 140 mM K-gluconate, pH 7.25 280 mOsm. Membrane potential was clamped at –60 or –70 mV. mEPSCs were recorded in the presence of 300–600 nM TTX and analyzed with the Minis Analysis program (Synaptosoft, Decatur, Georgia). Cultured neurons were prepared from E17.5–18.5 fetuses as previously described[48] (see Supplementary methods).

Note: Supplementary methods are available on the Nature Neuroscience web site (http://neuroscience.nature.com/web_specials).

Acknowledgements

We thank J. Plomp for advice and help in embryonic neuromuscular electrophysiology, S. Nixon for technical assistance, E. Padilla at the UNM-HSC Animal Resource Facility for maintaining the mouse colony and G. Adamson at the UC Davis EM Pathology lab for help with electron microscopy. We also thank P. De Camilli and A. Klip for antisera, and B. Shuttleworth and L. Anna Cunningham for discussions and for reading the manuscript. The work was supported by NIH MH 4-8989 (M.C.W.).

Competing interests statement

The authors declare that they have no competing financial interests.

RECEIVED 9 OCTOBER; ACCEPTED 26 NOVEMBER 2001

1. Katz, B. *The Release of Neural Transmitter Substances* (Liverpool University Press, Liverpool, 1969).
2. Young, S. & Poo, M. Spontaneous release of transmitter from growth cones of embryonic neurones. *Nature* **305**, 634–637 (1983).
3. Zakharenko, S., Chang, S., O'Donoghue, M. & Popov, S. V. Neurotransmitter secretion along growing nerve processes: comparison with synaptic vesicle exocytosis. *J. Cell Biol.* **144**, 507–518 (1999).
4. Söllner, T. *et al.* SNAP receptors implicated in vesicle targeting and fusion. *Nature* **362**, 318–324 (1993).
5. Brunger, A. Structural insights into the molecular mechanism of Ca^{2+}-dependent exocytosis. *Curr. Opin. Neurobiol.* **10**, 293–302 (2000).
6. Weber, T. *et al.* SNAREpins: minimal machinery for membrane fusion. *Cell* **92**, 759–772 (1998).
7. Schiavo, G., Matteoli, M. & Montecucco, C. Neurotoxins affecting neuroexocytosis. *Physiol. Rev.* **80**, 717–766 (2000).
8. Weimbs, T. *et al.* A conserved domain is present in different families of vesicular fusion proteins: a new superfamily. *Proc. Natl. Acad. Sci. USA* **94**, 3046–3051 (1997).
9. Deitcher, D. *et al.* Distinct requirements for evoked and spontaneous release of neurotransmitter are revealed by mutations in the *Drosophila* gene neuronal-synaptobrevin. *J. Neurosci.* **18**, 2028–2939 (1998).
10. Broadie, K. *et al.* Syntaxin and synaptobrevin function downstream of vesicle docking in *Drosophila*. *Neuron* **15**, 663–673 (1995).
11. Sweeney, S., Broadie, K., Keane, J., Niemann, H. & O'Kane, C. Targeted expression of tetanus toxin light chain in *Drosophila* specifically eliminates synaptic transmission and causes behavioral defects. *Neuron* **14**, 341–351 (1995).
12. Hua, S., Raciborska, D., Trimble, W. & Charlton, M. Different VAMP/synaptobrevin complexes for spontaneous and evoked transmitter release at the crayfish neuromuscular junction. *J. Neurophysiol.* **80**, 3233–3246 (1998).
13. Capogna, M., McKinney, R. A., O'Connor, V., Gahwiler, B. H. & Thompson, S. M. Ca^{2+} or Sr^{2+} partially rescues synaptic transmission in hippocampal cultures treated with botulinum toxin A and C, but not tetanus toxin. *J. Neurosci.* **17**, 7190–7202 (1997).
14. Verderio, C. *et al.* Tetanus toxin blocks the exocytosis of synaptic vesicles clustered at synapses but not of synaptic vesicles in isolated axons. *J. Neurosci.* **19**, 6723–6732 (1999).
15. Osen-Sand, A. *et al.* Inhibition of axon growth by SNAP-25 antisense oligonucleotides *in vitro* and *in vivo*. *Nature* **364**, 445–448 (1993).
16. Osen-Sand, A. *et al.* Common and distinct fusion proteins in axonal growth and transmitter release. *J. Comp. Neurol.* 222–234 (1996).
17. Morihara, T. *et al.* Distribution of synaptosomal-associated protein 25 in nerve growth cones and reduction of neurite outgrowth by botulinum neurotoxin A without altering growth cone morphology in dorsal root ganglion neurons and PC-12 cells. *Neuroscience* **91**, 695–706 (1999).
18. Coco, S. *et al.* Subcellular localization of tetanus neurotoxin-insensitive vesicle-associated membrane protein (VAMP)/VAMP7 in neuronal cells: evidence for a novel membrane compartment. *J. Neurosci.* **19**, 9803–9812 (1999).
19. Bark, I. C. Structure of the chicken gene for SNAP-25 reveals duplicated exons encoding distinct isoforms of the protein. *J. Mol. Biol.* **233**, 67–76 (1993).
20. Chapman, E. R., An, S., Barton, N. & Jahn, R. SNAP-25, a t-SNARE which binds to both syntaxin and synaptobrevin via domains that may form coiled coils. *J. Biol. Chem.* **269**, 27427–27432 (1994).
21. Sutton, R. B., Fasshauer, D., Jahn, R. & Brunger, A. T. Crystal structure of a SNARE complex involved in synaptic exocytosis at 2.4 A resolution. *Nature* **395**, 347–353 (1998).
22. Hess, D. T., Slater, T. M., Wilson, M. C. & Skene, J. H. P. The 25 kDa synaptosomal-associated protein SNAP-25 is the major methionine-rich polypeptide in rapid axonal transport and a major substrate for palmitoylation in adult CNS. *J. Neurosci.* **12**, 4634–4641 (1992).
23. Veit, M., Sollner, T. H. & Rothman, J. E. Multiple palmitoylation of synaptotagmin and the t-SNARE SNAP-25. *FEBS Lett.* **385**, 119–123 (1996).
24. Lane, S. R. & Liu, Y. Characterization of the palmitoylation domain of SNAP-25. *J. Neurochem.* **69**, 1864–1869 (1997).
25. Washbourne, P. *et al.* The cysteines of synaptosome-associated protein of 25 kDa (SNAP-25) are required for SNARE disassembly and exocytosis, not for membrane targeting. *Biochem. J.* **357**, 625–634 (2001).
26. Ravichandran, V., Chawla, A. & Roche, P. Identification of a novel syntaxin- and synaptobrevin/VAMP-binding protein, SNAP-23, expressed in non-neuronal tissues. *J. Biol. Chem.* **271**, 13300–13303 (1996).
27. Chen, D., Minger, S., Honer, W. & Whiteheart, S. Organization of the secretory machinery in the rodent brain: distribution of t-SNAREs SNAP-25 and SNAP-23. *Brain Res.* **831**, 11–24 (1999).
28. Verhage, M. *et al.* Synaptic assembly of the brain in the absence of neurotransmitter secretion. *Science* **287**, 864–869 (2000).
29. Ceccarelli, B. & Hurlbut, W. Ca^{2+}-dependent recycling of synaptic vesicles at the frog neuromuscular junction. *J. Cell Biol.* **87**, 297–303 (1980).
30. Capogna, M., Gahwiler, B. H. & Thompson, S. M. Calcium-independent actions of α-latrotoxin on spontaneous and evoked synaptic transmission in the hippocampus. *J. Neurophysiol.* **76**, 149–158 (1996).
31. Matteoli, M., Takei, K., Perin, M. S., Südhof, T. C. & De Camilli, P. Exoendocytotic recycling of synaptic vesicles in developing processes of cultured hippocampal neurons. *J. Cell. Biol.* **117**, 849–869 (1992).
32. del Castillo, J. & Katz, B. Quantal components of the end-plate potential. *J. Physiol. (Lond.)* **124**, 560–573 (1954).
33. Heuser, J. & Reese, T. Structural changes after transmitter release at the frog neuromuscular junction. *J. Cell Biol.* **88**, 564–580 (1981).
34. Mehta, P. P., Battenburg, E. & Wilson, M. C. SNAP-25 and synaptotagmin involvement in the final Ca^{+2}-dependent triggering of neurotransmitter exocytosis. *Proc. Natl. Acad. Sci. USA* **93**, 10471–10476 (1996).
35. Hayashi, T. *et al.* Synaptic vesicle membrane fusion complex: action of clostriridal neurotoxins on assembly. *EMBO J.* **13**, 5051–5061 (1994).
36. Pellegrini, L. L., O'Connor, V., Lottspeich, F. & Betz, H. Clostridal neurotoxins compromise the stability of a low energy SNARE complex mediating NSF activation of synaptic vesicle fusion. *EMBO J.* **14**, 4705–4713 (1995).
37. Yang, X. *et al.* Patterning of muscle acetylcholine receptor gene expression in the absence of motor innervation. *Neuron* **30**, 399–410 (2001).
38. Lin, W. *et al.* Distinctive roles of nerve and muscle in postsynaptic differentiation of the neuromuscular synapse. *Nature* **410**, 1057–1064 (2001).
39. Geppert, M. *et al.* Synaptotagmin I: a major Ca^{2+} sensor for transmitter release at a central synapse. *Cell* **79**, 717–727 (1994).
40. Dulubova, I. *et al.* A conformational switch in syntaxin during exocytosis: role of munc18. *EMBO J.* **18**, 4372–4382 (1999).
41. Schiavo, G., Stenbeck, G., Rothman, J. E. & Sollner, T. H. Binding of the synaptic vesicle v-SNARE, synaptotagmin, to the plasma membrane t-SNARE, SNAP-25, can explain docked vesicles at neurotoxin-treated synapses. *Proc. Natl. Acad. Sci. USA* **94**, 997–1001 (1997).
42. McKinney, R. A., Capogna, M., Durr, R., Gahwiler, B. H. & Thompson, S. M. Miniature synaptic events maintain dendritic spines via AMPA receptor activation. *Nat. Neurosci.* **2**, 44–49 (1999).
43. Schoch, S. *et al.* SNARE function analyzed in synaptobrevin/VAMP knockout mice. *Science* **294**, 1117–1122 (2001).
44. Mansour, S. L., Thomas, K. R. & Capecchi, M. R. Disruption of the proto-oncogene int-2 in mouse embryo-derived stem cells: a general strategy for targeting mutations to non-selectable genes. *Nature* **336**, 348–352 (1988).
45. Gautam, M. *et al.* Defective neuromuscular synaptogenesis in agrin-deficient mutant mice. *Cell* **85**, 525–535 (1996).
46. Plomp, J., van Kempen, G. & Molenaar, P. Adaptation of quantal content to decreased postsynaptic sensitivity at single endplates in α-bungarotoxin-treated rats. *J. Physiol. (Lond.)* **458**, 487–499 (1992).
47. Aitken, P. G. *et al.* Preparative methods for brain slices: a discussion. *J. Neurosci. Methods.* **59**, 139–149 (1995).
48. Costa, E., Soto, E., Cardoso, R., Olivera, D. & Valenzuela, C. Acute effects of ethanol on kainate receptors in cultured hippocampal neurons. *Alcohol Clin. Exp. Res.* **24**, 220–225 (2000).